

Optimal Power Allocations for Full-Duplex Enhanced Visible Light Communications

Liping Liang, Wenchi Cheng^(✉), and Hailin Zhang

State Key Laboratory of Integrated Services Networks,
Xidian University, Xi'an, China
lpliang@stu.xidian.edu.cn,
{wccheng, hlzhang}@xidian.edu.cn

Abstract. We consider the two nodes indoor full-duplex transmission over bidirectional channels with imperfect self-interference cancellation in visible light communications (VLCs). The light emitting diodes (LEDs) are used for illumination and data transmission while the photo diodes (PDs) are used for reception. In this paper, we first formulate the sum-capacity maximization problem for the full-duplex bidirectional VLCs. Then, we develop an optimal power allocation scheme, which has the closed-form expression, to achieve the maximum sum-capacity for two nodes indoor full-duplex bidirectional VLCs. The obtained numerical results verify our developed optimal power allocation scheme and show that the full-duplex transmission can significantly increase the sum-capacity than the traditional half-duplex transmission.

Keywords: Visible light communications · Full-duplex · Bidirectional transmission · Power allocations · Self-interference · Sum-capacity

1 Introduction

The optical wireless communication, which can efficiently overcome the spectrum deficiency problem in radio communications, has attracted a lot of attention in past few years. It has been shown that the optical wireless communications can be applied in transdermal communications, transports, mobile medical body area networks, underwater communications, and indoor optical wireless communications [1–4]. Among various optical wireless communications, the VLC rapidly emerges as an attractive communication technology [1]. Visible light communication uses visible light spectrum in the range of wavelength 380–780 nm, which is license-free and does not generate the electromagnetic interference to the existing radio frequency (RF) systems. In VLC systems, white light emitting diodes (LEDs) are used for illumination as well as the signal transmitter while photo diodes (PDs) are used as the receiver. The LEDs

This work was supported in part by the National Natural Science Foundation of China (No. 61401330), the 111 Project of China (B08038), and the Natural Science Foundation of Shaanxi Province (No. 2016JQ6027).

can support cable free communications as high as several tens Mbps between the LEDs and the PDs [5].

In half-duplex VLC systems, we need two time-slots to communicate between the two nodes, resulting in low network throughput. To deal with this issue, we propose to use full-duplex VLCs in this paper. The full-duplex wireless communication holds the promise of double spectral efficiency, compared with the traditional half-duplex wireless communication [6, 7], through simultaneous transmission and reception using the same frequency band at the same time. The wireless full-duplex communication mode was thought to be unfeasible because of the very large self-interference leaked from the local transmitter to the local receiver, thus making it difficult to extract the useful receive signal transmitted from the other node. Therefore, it is critical to be able to limit the power of the self-interference to implement full-duplex communications in practice. Recently, a great number of research works have shown the possibility of using full-duplex transmission in wireless communications using advanced propagation-domain interference suppression, analog-domain interference cancelation, and digital-domain interference cancelation [8–12]. Taking the self-interference as a part of useful information, the authors of [13] applied the full-duplex relay VLC based system to mitigate the self-interference. Some researchers proposed a self-adaptive minimum contention window full-duplex MAC protocol to mitigate channel collisions for VLCs [14]. To employ the full-duplex capacity efficiently, the paper [15] proposed two contention protocols, named UALOHA and FD-CSMA. The authors of [16] proved that the average electrical SNR per transmit antenna is considerably high in indoor MIMO optical wireless communications.

In this paper, we consider the two nodes full-duplex bidirectional transmission under imperfect self-interference cancelation in VLCs. We develop an optimal power allocation scheme to maximize the sum-capacity of two nodes visible light full-duplex bidirectional transmission for VLCs. For visible light full-duplex transmission in high signal-to-interference-noise rate (SINR) region, we derive the closed-form expression of optimal power allocation scheme.

The rest of this paper is organized as follows. Section 2 describes the system model. Section 3 formulates sum-capacity maximization problem for the full-duplex VLCs. Section 4 develops the optimal power allocation scheme in the high SINR region for visible light full-duplex bidirectional transmission. Section 5 carries out the numerical results to evaluate our developed optimal power allocation scheme and the achieved sum-capacity for two nodes visible light full-duplex bidirectional transmission compared with the traditional half-duplex transmission. Section 6 concludes the paper.

2 The System Model

In this paper, we consider the two nodes wireless full-duplex bidirectional visible light communications, as illustrated in Fig. 1, where node A and node B transmit their data to node B and node A, respectively. Each node is equipped with LEDs and PDs. The LEDs are used for both illumination and transmission while the PDs are used for reception. The optical modulation and demodulation schemes are set as intensity

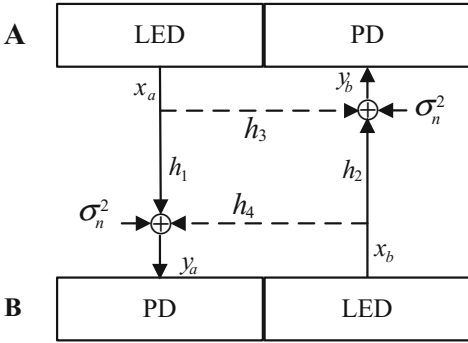


Fig. 1. The two nodes full-duplex bidirectional transmission in VLCs.

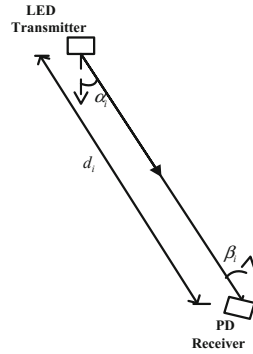


Fig. 2. The geometry of a transmitter-receiver pair.

modulation (IM) and direct detection (DD). The channels from node A to node B and from node B to node A use the same frequency band at the same time.

The shot and thermal noise in the receiver are modeled as additive white Gaussian noise (AWGN) and are added to the signal in the electrical domain. Thus, we have the total noise variance as $\sigma_n^2 = \sigma_{\text{shot}}^2 + \sigma_{\text{thermal}}^2$, where σ_{shot}^2 is the shot noise variance and $\sigma_{\text{thermal}}^2$ is the thermal noise variance [17]. We assume that all total noise variances are the same and uniformly denoted by σ_n^2 for mathematical simplification. We assume that the optical signal propagates from the transmitter to the receiver directly (Light of Sight) and the reflections are ignored [16]. We denote by h_1^2 and h_2^2 the channel gains from node A to node B and from node B to node A, respectively. We denote by h_3^2 and h_4^2 the self-interference channel gains from local transmitter to local receiver at nodes A and B, respectively. For one transmitter-receiver pair as shown in Fig. 2, the h_i ($i = 1, 2, 3, 4$) is given by

$$h_i = \begin{cases} \frac{(m+1)A}{2\pi d_i^2} \cos^m(\alpha_i) \cos^\gamma(\beta_i) & \text{if } \alpha_i, \beta_i \in (0, \frac{\pi}{2}); \\ 0 & \text{others,} \end{cases} \quad (1)$$

where m is the Lambertian emission order and given as follow (We assume that there is only one Lambertian emitting mode for LED):

$$m = \frac{-\ln 2}{\ln(\cos \psi_{1/2})}. \quad (2)$$

The parameter $\psi_{1/2}$ is the semi-angle of the LED at half-power. In Eq. (1), A is the active area of PD and γ is the filed-of-view (FoV) coefficient of the PD receiver [18]. For the i th channel (h_i), d_i , α_i and β_i ($i = 1, 2, 3, 4$) are the distance from LED to PD, the irradiance angle at LED, and the incident angle at PD, respectively. We denote by P_a and P_b the transmitter power at nodes A and B, respectively.

To evaluate the performance of visible light full-duplex bidirectional transmission, we employ the concept of capacity region [19]. The capacity region for two nodes visible light full-duplex transmission is defined as the set of rate pairs (R_A, R_B) such that the transmitters of node A and node B can reliably transmit data to the receivers of node B and node A simultaneously, where R_A and R_B denote the channel rates from node A to node B and from node B to node A, respectively. Because node A and node B share the same bandwidth, there is a tradeoff between the reliable communication rates R_A and R_B . $R_A(R_B)$ increases as $R_B(R_A)$ decreases. The received signal at nodes A and B, denoted by \mathbf{y}_b and \mathbf{y}_a , respectively, can be derived as follows:

$$\begin{cases} \mathbf{y}_a = \sqrt{P_a}h_1\mathbf{x}_a + \sqrt{P_b}h_4\mathbf{x}_b + \sigma_n^2; \\ \mathbf{y}_b = \sqrt{P_b}h_3\mathbf{x}_a + \sqrt{P_a}h_2\mathbf{x}_b + \sigma_n^2, \end{cases} \quad (3)$$

where \mathbf{x}_a and \mathbf{x}_b represent the transmitted signal at nodes A and B, respectively, as illustrated in Fig. 1. Then, we define the sum-capacity as the scalar performance measure to evaluate the two nodes visible light full-duplex bidirectional transmission. The sum-capacity for two nodes visible light full-duplex bidirectional transmission, denoted by \mathbf{s}_b , is formulated as follows:

$$\mathbf{s}_b = \mathbf{y}_a + \mathbf{y}_b. \quad (4)$$

3 The Sum-Capacity Maximization Problem Formulation

For the wireless full-duplex bidirectional transmission, there still exists the residue self-interference even the advanced self-interference mitigation schemes are applied [8–12]. To characterize self-interference in visible light full-duplex bidirectional transmission, this section introduces a parameter κ ($0 \leq \kappa \leq 1$), which is defined as the self-interference mitigation coefficient. Then based on self-interference mitigation coefficient, we can build up the received residue self-interference model, denoted by $f(P_t, h, x_t)$ as follows:

$$f(P_t, h, x_t) = \sqrt{\kappa P_t} h x_t, \quad (5)$$

where x_t , h , and P_t represent the local transmit signal, the channel gain from the local transmitter to the local receiver, and the transmit power, respectively. Based on Eq. (5), it is clear that self-interference decreases with self-interference mitigation coefficient κ decreases. When $\kappa = 1$, self-interference mitigation technique does not work. When $\kappa = 0$, it indicates that self-interference between the local transmitter and the local receiver can be completely canceled. In fact, $\kappa = 0$ is impossible using the current techniques.

We assume that all self-interference mitigation coefficients are the same and uniformly denoted by κ for mathematical simplification. Then, the received signal at nodes A and B, denoted by \mathbf{y}_b and \mathbf{y}_a , respectively, can be formulated as follows:

$$\begin{cases} \mathbf{Y}_a = \sqrt{P_a}h_1\mathbf{x}_a + f(\sqrt{P_b}, h_4, \mathbf{x}_b) + \sigma_n^2 = \sqrt{P_a}h_1\mathbf{x}_a + \sqrt{\kappa P_b}h_4\mathbf{x}_b + \sigma_n^2; \\ \mathbf{Y}_b = \sqrt{P_b}h_2\mathbf{x}_b + f(\sqrt{P_a}, h_3, \mathbf{x}_a) + \sigma_n^2 = \sqrt{P_b}h_2\mathbf{x}_b + \sqrt{\kappa P_a}h_3\mathbf{x}_a + \sigma_n^2. \end{cases} \quad (6)$$

We denote by $SINR_a$ and $SINR_b$ the SINRs of the received signal Y_a and Y_b . Then, based on the analyses above, $SINR_a$ and $SINR_b$ can be expressed as follows:

$$\begin{cases} SINR_a = \frac{P_a h_1^2}{\sigma_n^2 + \kappa P_b h_4^2}; \\ SINR_b = \frac{P_b h_2^2}{\sigma_n^2 + \kappa P_a h_3^2}. \end{cases} \quad (7)$$

The capacity from node A to node B and from node B to node A, denoted by $C_{ab}(P_a, P_b)$ and $C_{ba}(P_a, P_b)$, respectively, can be derived as follows:

$$\begin{cases} C_{ab} = \log(1 + SINR_a); \\ C_{ba} = \log(1 + SINR_b). \end{cases} \quad (8)$$

Thus, we can derive the achievable sum-capacity of two nodes optical wireless full-duplex bidirectional transmission, denoted by $C_B(P_a, P_b)$, as follows:

$$C_B(P_a, P_b) = C_{ab}(P_a, P_b) + C_{ba}(P_a, P_b) = \log(1 + SINR_a) + \log(1 + SINR_b). \quad (9)$$

Our goal aims at allocating the transmit power to achieve the maximum sum-capacity for two nodes optical wireless full-duplex bidirectional transmission. Then, we can formulate the sum-capacity maximization problem, denoted by \mathbf{PI} , as follows:

$$\mathbf{PI} : \arg \max_{(P_a, P_b)} \{C_B(P_a, P_b)\} \quad (10)$$

$$\text{s.t. : (1) } P_a > 0, P_b > 0; \quad (11)$$

$$(2) P_a + P_b \leq \bar{P}, \quad (12)$$

where \bar{P} represents the average power constraint. Observing $C_B(P_a, P_b)$ specified in Eq. (9), we know that the capacity $C_B(P_a, P_b)$ is a nonconcave function over the space spanned by (P_a, P_b) . Thus, \mathbf{PI} is not a strictly convex optimization problem. To obtain the maximum capacity $C_B(P_a, P_b)$, it is desirable that \mathbf{PI} is a strictly convex optimization problem. In the following section, we convert \mathbf{PI} to convex optimization problem and develop the optimal power allocation scheme to obtain the global optimal solution for \mathbf{PI} .

4 The Optimal Power Allocation Scheme in the High SINR Region

In the high SINR region, $C_B(P_a, P_b)$ can be re-written as follows:

$$\begin{aligned}
 C_B(P_a, P_b) &= \log\left(\frac{P_a h_1^2}{\sigma_n^2 + \kappa P_b h_4^2}\right) + \log\left(\frac{P_b h_2^2}{\sigma_n^2 + \kappa P_a h_3^2}\right) \\
 &= \log\left(\frac{P_a P_b h_1^2 h_2^2}{\sigma_n^4 + \sigma_n^2 \kappa P_a h_3^2 + \sigma_n^2 \kappa P_b h_4^2 + \kappa^2 P_a P_b h_3^2 h_4^2}\right).
 \end{aligned} \tag{13}$$

Because $\log(\bullet)$ is a monotonically increasing function as the independent variables increase, we can convert the problem **P1** to a new problem **P2**, which is an equivalent problem as **P1** and can be expressed as follows:

$$\mathbf{P2} : \max_{(P_a, P_b)} \left(\frac{P_a P_b h_1^2 h_2^2}{\sigma_n^4 + \sigma_n^2 \kappa P_a h_3^2 + \sigma_n^2 \kappa P_b h_4^2 + \kappa^2 P_a P_b h_3^2 h_4^2} \right) \tag{14}$$

subject to the constraints given in Eqs. (11) and (12). Then we have the Lemma 1 as follows:

Lemma 1: The problem **P2** is a strictly convex optimization problem.

Proof: We define the function $f(P_a, P_b)$ as follows:

$$f(P_a, P_b) = \frac{h_1^2 h_2^2}{\frac{\sigma_n^4}{P_a P_b} + \frac{\sigma_n^2 \kappa h_3^2}{P_b} + \frac{\sigma_n^2 \kappa h_4^2}{P_a} + \kappa^2 h_3^2 h_4^2}. \tag{15}$$

Since $(\sigma_n^4/P_a P_b + \sigma_n^2 \kappa h_3^2/P_b + \sigma_n^2 \kappa h_4^2/P_a + \kappa^2 h_3^2 h_4^2)$ decreases as P_a and P_b increase, $(\sigma_n^4/P_a P_b + \sigma_n^2 \kappa h_3^2/P_b + \sigma_n^2 \kappa h_4^2/P_a + \kappa^2 h_3^2 h_4^2)$ is strictly convex on the space spanned by (P_a, P_b) when P_a and P_b are subject to the constraints given in Eqs. (11) and (12). Thus, $f(P_a, P_b)$ is a strictly concave function on the space spanned by (P_a, P_b) . On the other hand, it is clear to verify that all inequalities constraints (Eqs. (11) and (12)) are linear on the space spanned by (P_a, P_b) . Therefore, the problem **P2** is a strictly convex optimization problem. To derive the optimal solutions of the problem **P2**, we have the following Theorem 1.

Theorem 1: The optimal solutions to the problem **P2**, denoted by P_a^* and P_b^* , are determined by

$$\begin{cases} P_a^* = \frac{\sigma_n^2 + \kappa \bar{P} h_4^2 - \sqrt{(\sigma_n^2 + \kappa \bar{P} h_4^2)^2 - \kappa (h_4^2 - h_3^2) (\bar{P} \sigma_n^2 + \kappa \bar{P}^2 h_4^2)}}{\kappa (h_4^2 - h_3^2)}; \\ P_b^* = \frac{-\sigma_n^2 - \kappa \bar{P} h_3^2 + \sqrt{(\sigma_n^2 + \kappa \bar{P} h_4^2)^2 - \kappa (h_4^2 - h_3^2) (\bar{P} \sigma_n^2 + \kappa \bar{P}^2 h_4^2)}}{\kappa (h_4^2 - h_3^2)}. \end{cases} \tag{16}$$

Proof: Because problem **P2** is a strictly convex optimization problem, it has the unique optimal solution. It is easy to know that the optimal solutions to problem **P2** need to satisfy $P_a^* + P_b^* = \bar{P}$. Thus, the optimal solution P_a^* and P_b^* need to satisfy

$$\begin{cases} \frac{\partial f(P_a, P_b)}{\partial P_a} = \frac{\sigma_n^4(\bar{P}-2P_a)h_1^2h_2^2 - \sigma_n^2P_a^2\kappa h_1^2h_2^2h_3^2 + \sigma_n^2(\bar{P}-P_a)^2\kappa h_1^2h_2^2h_4^2}{(\sigma_n^4 + \sigma_n^2\kappa P_a h_3^2 + \sigma_n^2\kappa P_b h_4^2 + \kappa^2 P_a P_b h_3^2 h_4^2)^2}; \\ \frac{\partial f(P_a, P_b)}{\partial P_b} = \frac{\sigma_n^4(\bar{P}-2P_b)h_1^2h_2^2 - \sigma_n^2P_b^2\kappa h_1^2h_2^2h_4^2 + \sigma_n^2(\bar{P}-P_b)^2\kappa h_1^2h_2^2h_3^2}{(\sigma_n^4 + \sigma_n^2\kappa P_a h_3^2 + \sigma_n^2\kappa P_b h_4^2 + \kappa^2 P_a P_b h_3^2 h_4^2)^2}; \\ (P_a^* + P_b^*) - \bar{P} = 0; \\ P_j^* > 0, j \in \{a, b\}. \end{cases} \quad (17)$$

Solving Eq. (17), we can derive the optimal solution expressed as shown in Eq. (16). Thus, Theorem 1 follows.

Theorem 1 gives the expression of the optimal solutions P_a^* and P_b^* in the high SINR region. The solutions are very accurate in the high SINR region and have the simple closed-form expression.

5 Numerical Results

In this section, we conduct numerical results to evaluate the performance of our developed optimal power allocation scheme for the visible light full-duplex bidirectional transmission. We consider a $4\text{ m} \times 4\text{ m} \times 3\text{ m}$ space. We assume that the LEDs are Lambertian sources with the semi-angle at half power $\psi_{1/2} = 60^\circ$ (which determines $m = 1$). We further assume that the average power constraint \bar{P} is set as 70 W. We set $A = 15\text{ mm}^2$ smaller than 1 cm^2 and $\gamma = 1.4738$ [16].

Figure 3 depicts the developed power allocation scheme for the two nodes visible light full-duplex transmission, where we set the irradiance angle at LED (α_i) as 15° and the incident angle at PD (β_i) as 30° ($i = 1, 2, 3, 4$). As shown in Fig. 3, when the distance (h_3) from the local transmitter to the local receiver at node A is very closed to distance (h_4) from the local transmitter to the local receiver at node B, the optimal power P_a^* and P_b^* are almost half of the average power. The optimal power of node A increases as h_3 decreases and h_4 increases. The optimal power of node B increases as h_3

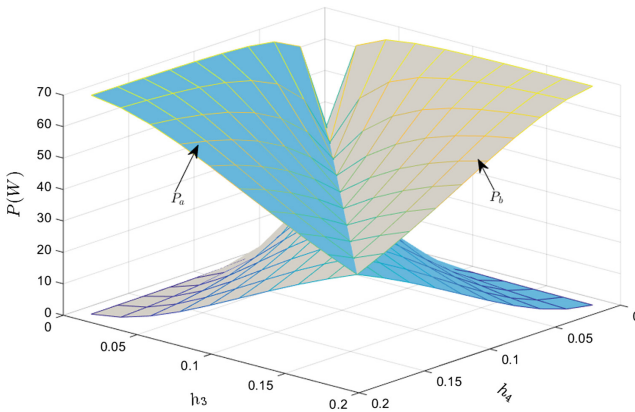


Fig. 3. The power allocations versus the distances from local transmitters to local receivers.

increases and h_4 decreases. This result proves that the visible light full-duplex transmission can be well applied because the large self-interference has been efficiently mitigated in the high SINR region.

Figure 4 evaluates the sum-capacity of using our developed optimal full-duplex power allocation scheme and the half-duplex scheme with different irradiance angle at LEDs and different incident angle at PDs, where we set distances from the transmitter of node A to the receiver of node B and from the transmitter of node B to the receiver of node A as 0.9 m and 0.5 m, respectively. We assume that the irradiance angle at LEDs and the incident angle at PDs from local LEDs to local PDs for node A and node B are set as 15° and 30° , respectively. The irradiance angle at LEDs and the incident angle at PDs from node A to node B and from node B to node A are set as the same size, i.e., $\alpha_1 = \alpha_2$ and $\beta_1 = \beta_2$. Thus, we can obtain the result that the sum-capacity decreases as irradiance angle at LEDs and incident angle at PDs increase. As we expected, the sum-capacity of using our optimal full-duplex power allocation scheme is much larger than the traditional half-duplex scheme except the scenario that both irradiance angle at LEDs and incident angle at PDs are very closed to 90° . The ideal case is that the LEDs are always oriented to the PDs, i.e., $\alpha_i = 0^\circ$ and $\beta_i = 0^\circ$ ($i = 1, 2$). Under this case, we have the maximum sum-capacity for the full-duplex VLCs.

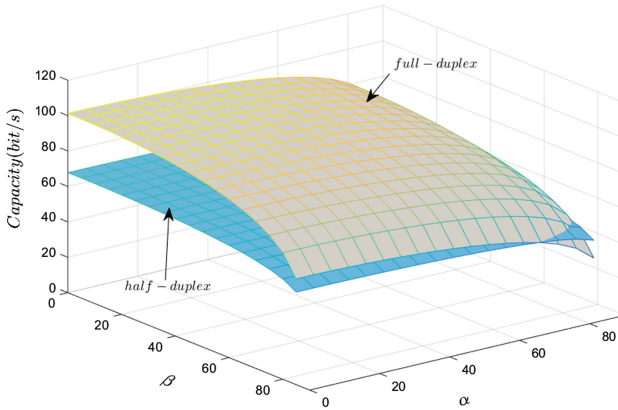


Fig. 4. The sum-capacity of using our developed optimal full-duplex power allocation scheme and the half-duplex scheme versus different irradiance angle at LEDs and different incident angle at PDs.

Figure 5 depicts the sum-capacity of using our optimal full-duplex power scheme and the half-duplex scheme with different d and different κ . The distances from the local transmitter to the local receiver at nodes A and B are set as 0.08 m and 0.1 m, respectively. The irradiance angle at LED (α_i) and the incident angle at PD (β_i) are set as the same as those in Fig. 3 ($i = 1, 2, 3, 4$). As shown in Fig. 5, we obtain that the sum-capacity of both visible light full-duplex and half-duplex transmission decreases as d and κ increases. The sum-capacity of using our optimal full-duplex power allocation scheme is nearly twice compared with that of the half-duplex scheme except the case that the distance between the two nodes is closed to 4 m and κ is considerably small.

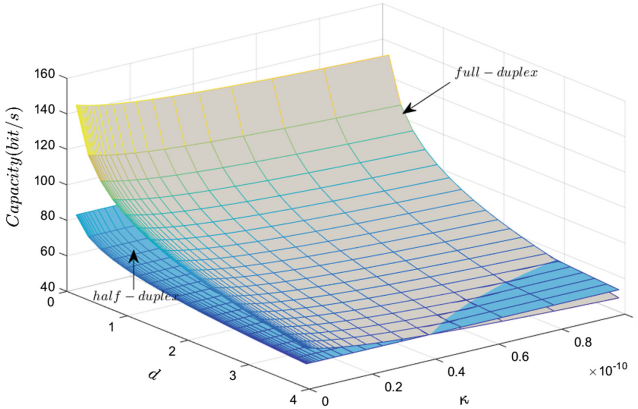


Fig. 5. The sum-capacity of using our developed optimal full-duplex power allocation scheme and the half-duplex scheme versus κ and d .

As self-interference mitigation coefficient (κ) increases, the sum-capacity of using the optimal visible light full-duplex power allocation scheme is larger than the half-duplex scheme under the condition that d is not very closed to 4 m. The other case is that d approximates to 4 m, there is a critical value κ_{th} of the sum-capacity between the full-duplex transmission and the half-duplex transmission. If self-interference mitigation coefficient (κ) is smaller than κ_{th} , the full-duplex power allocation scheme achieves larger sum-capacity than the half-duplex transmission. Observing Figs. 4 and 5, we find that the sum-capacity of using our developed optimal power allocation scheme in visible light full-duplex bidirectional transmission is larger than the sum-capacity in traditional half-duplex transmission with different κ , different distance d between the two nodes, different self-interference mitigation coefficient κ , different irradiance angle at LEDs, and different incident angle at PDs in most cases in the high SINR region.

6 Conclusions

In this paper, we built up the model to analyze the two nodes full-duplex bidirectional transmission in VLCs. Based on this model, we developed the optimal power allocation scheme to maximize the sum-capacity of two nodes visible light full-duplex bidirectional transmission. In high SINR region, we obtained the maximum sum-capacity of two nodes with different distance from the local transmitter to the local receiver, different distance between the two nodes, different self-interference mitigation coefficient, different irradiance angle at LEDs, and different incident angle at PDs. The numerical results show that visible light full-duplex transmission can significantly increase the sum-capacity than the traditional half-duplex transmission.

References

1. Arnon, S., Uysal, M., Ghassemlooy, Z., Xu, Z., Cheng, J.: Guest editorial optical wireless communications. *IEEE J.* **33**, 1733–1737 (2015)
2. Sanz, M.G.: Visible light data communications. Project, Dept. of Electronics and Electrical Engineering, University of Glasgow, UK (2011–2012), <http://www.glasgow.ac.uk/engineering>
3. Elgala, H., Mesleh, R., Haas, H.: Indoor optical wireless communications: potential and State-of-the-art. *IEEE Commun. Mag.* **49**(9), 56–62 (2011)
4. Tsonev, D., Sinaovic, S., Hass, H.: Practical MIMO capacity for indoor optical wireless communication with white LEDs. In: *Proceedings of IEEE VTC-Spring*, New York, pp. 1–5 (2013)
5. Bouchet, O.: Visible-light communication system enabling 73 Mb/s data streaming. In: *IEEE GLOBECOM 2010 Workshop on Optical Wireless Communications*, Miami, Florida (2010)
6. Bliss, D.W., Parker, P.A., Margetts, A.R.: Simultaneous transmission and reception for improved wireless network performance. In: *IEEE Workshop Statistics and Signal Process*, pp. 478–482 (2007)
7. Riihonen, T., Werner, S., Wichman, R.: Comparison of full-duplex and half-duplex modes with a fixed amplify-and-forward relay. In: *IEEE Wireless Communications and Networking Conference*, pp. 1–5 (2009)
8. Choi, J.I., Jain, M., Srinivasan, K., Levis, P., Katti, S.: Achieving single channel, full duplex wireless communication. In: *Proceedings of 16th ACM MOBICOM*, Chicago, Illinois, USA (2010)
9. Jain, M., Chio, J.I., Kim, T.M., Bharadia, D., Seth, S., Srinivasan, K., Levis, P., Katti, S., Sinha, P.: Practical, real-time, full duplex wireless. In: *Proceedings of 17th ACM MOBICOM*, Las Vegas, Nevada, USA (2011)
10. Duarte, M., Sabharwal, A.: Full-duplex wireless communications using off-the-shelf radios: feasibility and first results. In: *Proceedings of Annual Asilomar Conference on Signals, Systems and Computers*, pp. 1558–1562 (2011)
11. Bozidar, R., Dinan, R., Peter, K., Alexandre, P., Nikhil, S., Vlad, B., Gerald, D.: Rethinking indoor wireless mesh design: low power, low frequency, full-duplex. In: *5th IEEE Workshop on Wireless Mesh Networks (WIMESH 2010)*, pp. 1–6 (2010)
12. Everett, E., Duarte, M., Dick, C., Sabharwal, A.: Empowering full-duplex wireless communication by exploiting directional diversity. In: *45th Asilomar Conference on Signals, Systems and Computers*, pp. 2002–2006 (2011)
13. Yang, H., Pandharipande, A.: Full-duplex relay VLC in LED lighting linear system topology. In: *IECON 39th Annual Conference of the IEEE*, pp. 6075–6080 (2013)
14. Wang, Z., Liu, Y., Lin, Y., Huang, S.: Full-duplex MAC protocol based on adaptive contention window for visible light communication. *IEEE/OSA J. Opt. Commun. Netw.* **7**, 164–171 (2015)
15. Zhang, Z., Yu, X., Wu, L., Dang, J., Li, V.O.K.: Performance analysis of full-duplex visible light communication networks. In: *ICC*, pp. 3933–3938 (2015)
16. Nuwanpriya, A., Ho, S., Chen, C.S.: Indoor MIMO visible light communications: novel angle diversity receivers for mobile users. *IEEE J.* **33**, 1780–1792 (2015)
17. Fath, T., Haas, H.: Performance comparison of MIMO techniques for optical wireless communications in indoor environments. *IEEE Trans. Commun.* **61**(2), 733–742 (2013)

18. Yang, S.-H., Jung, E.-M., Han, S.-K.: Indoor location estimation based on LED visible light communication using multiple optical receivers. *IEEE Commun. Lett.* **17**(9), 1834–1837 (2013)
19. Cheng, W., Zhang, X., Zhang, H.: Optical dynamic power control for full-duplex bidirectional-channel based wireless networks. In: *Proceedings of IEEE INFOCOM*, pp. 3120–3128 (2013)